Multi-objective design optimization of five-phase fractional-slot concentrated-winding surface-mounted permanent-magnet machine

AMIR NEKOUBIN[ID], JAFAR SOLTANI, MILAD DOWLATSHAH

Department of Electrical Engineering, Islamic Azad University Khomeinishahr Branch
Khomeinishahr/Isfahan, Iran
e-mails: nekoubin@yahoo.com, {jafar.soltanizamani/milad.dowlatshahi}@gmail.com

Abstract: The multi-phase permanent-magnet machines with a fractional-slot concentrated-winding (FSCW) are a suitable choice for certain purposes like aircraft, marine, and electric vehicles, because of the fault tolerance and high power density capability. The paper aims to design, optimize and prototype a five-phase fractional-slot concentrated-winding surface-mounted permanent-magnet motor. To optimize the designed multi-phase motor a multi-objective optimization technique based on the genetic algorithm method is applied. The machine design objectives are to maximize torque density of the motor and maximize efficiency then to determine the best choice of the designed machine parameters. Then, the two-dimensional Finite Element Method (2D-FEM) is employed to verify the performance of the optimized machine. Finally, the optimized machine is prototyped. The paper found that the results of the prototyped machine validate the results of theatrical analyses of the machine and accurate consideration of the parameters improved the acting of the machine.

Key words: Finite Element Method, genetic algorithm, optimization, permanent-magnet motors

1. Introduction

A multi-phase motor has several advantages that make this motor preferable to three-phase motors. Multiphase motors can operate under fault condition by using the healthy phases [1–5]. The ability to reduce amplitude and boost the frequency of torque ripple, and the minimization of the stator current per phase without developing the voltage per phase, are the other merits of multiphase motors [6–8]. By adding a number of phases, it is also feasible to develop the torque

per RMS ampere for the same volume machine [9, 10]. A multiphase motor is a suitable choice for use where high reliability is needed such as in aircraft, marine, and electric vehicles [11, 12].

Permanent magnet synchronous motors with fractional-slot concentrated windings have higher slot fill factor and lower end windings. In addition, the phase's mutual inductances are decreased remarkably. These features enhance the power density of the machine and efficiency. Further, cogging torque will be diminished [3].

Sadeghi [13], have introduced an optimal design of a five-phase Halbach permanent-magnet motor in order to achieve high efficiency, high torque, and high acceleration. The proposed optimal design is validated through finite-element analysis. It is shown that the optimized multi-phase permanent magnet machine offers good performance. The effects of different design variables on torque ripple and torque linearity that should be investigated at the design stage is studied in [14], it is concluded that torque ripple and torque linearity will be improved by reducing electrical loading.

In [15] a five-phase fault-tolerant permanent magnet synchronous machine (PMSM) for electric vehicles is investigated and, for getting sinusoidal back-electromotive force (EMF), two typical methods consisting of rotor eccentricity and a Halbach permanent-magnet array are studied and compared. Also, a PM method is proposed to decrease PM eddy current loss, it is seen that after PM segmentation, the eddy current loss is reduced significantly. In [16] a FEM model is used to optimize the radius of the magnet with a mention to the number of poles, rotor size, and magnet thickness. Features of a permanent-magnet synchronous motor (PMSM) are affected significantly by the back-electromotive force waveforms in the motor, which are directly dependent on magnet shape, it is seen that the optimized motor produces very low total harmonic distortion.

In [17] a new surrogate-assisted multi-objective optimization algorithm is introduced. The introduced algorithm is employed to an optimal design process of a three-phase IPM motor to decrease the noise, vibration, and cost. It is seen that, the introduced algorithm can reduce the design time and effort in IPM motors design using FEM analysis.

In another study [18], the new design optimization technique of interior permanent magnet (IPM) synchronous motors based on the Finite Element Method is presented. The presented optimization technique is implemented to design two IPM motors for an industrial city electric scooter. It is observed that the simulation results are effective and confirm the proposed technique.

In [19] a single objective optimization to maximize the torque density for a three- phase surface-mounted PM motor is applied. In this work, discontinuous variables such as determination of steel type, permanent-magnet (PM) type, and conductor type are also regarded. It is found that, the optimized motor produces high torque density. Multi-objective genetic algorithms consist of two types, non-elitist and elitist [20]. The elitist strategies are completely applicable because they effectively identify and retain the non-dominated individuals [21]. In [22] simulation of a 5-phase PM motor with a trapezoidal back-EMF is done. To minimize copper losses a new control technique is proposed and experimentally verified. It is seen that, the proposed method has suitable performance for multi phase motors.

In [23] an IPM motor with a five-phase and fractional-slot stator is investigated. It is seen that the presented five-phase motor with a fractional slot produces lower torque ripple. In [24] a design model of a three-phase surface-mounted PM motor is presented. The proposed model is suitable to be employed for optimal machine design. There is extra attention to the optimized design of PM motors using a genetic algorithm (GA).

To promote the performance of multi-phase machine design optimization of the machine is necessary. In this work, the elitist non-dominated sorting GA (NSGA-II) strategy is employed to optimize the multi-phase PM machine [25]. Then, the optimized machine is verified by an FEM model. Finally, the optimized five-phase, surface-mounted PM machine (SPMSM) is prototyped. Thus, the main contributions of this paper are:

1) to design and optimize multi-objectively a five-phase FSCW motor based on the NSGA-II strategy to maximize torque density of the motor, maximize efficiency and determination the best choice of the designed machine parameters;

2) two-dimensional Finite Element Method (2D-FEM) analysis to attest the acting of the optimized motor;

3) prototyping an FSCW 20-slot/22-pole five-phase, surface-mounted PM machine (SPMSM).

The analytical design and results are introduced in the second section. In the third section, the designed machine is optimized multi-objectively. In the fourth section, 2D-FEM analysis of the optimized machine is done then it is prototyped and experimental results are presented.

2. Design of five-phase PMSM motor

The winding factors and MMF harmonic components of an FSCW motor are mainly indicated by slot/pole combination. Also, other chrectrestics of the motor like ripple torque, net radial force and rotor loss, are affected. Hence, determining an optimized slot/pole combination is fundamental in the motor design steps. The main component of winding factors for possible slot/pole combination of a 5-phase machine is computed and shown in Table 1.

Table 1. Main winding factors of the multi-phase motor

s/p	2	4	6	8	12	14	16	18	20	22	24
5	0.58	0.951	0.95	0.58	0.58	0.95	0.95	0.58	–	0.58	0.95
10	–	0.58	0.80	0.95	0.95	0.80	0.58	0.30	–	0.30	0.58
15	0.20	0.40	0.58	0.73	0.95	0.98	0.98	0.95	–	0.73	0.58
20	–	–	0.44	0.58	0.80	0.88	0.95	0.97	–	0.975	0.95
25	0.12	0.24	0.36	0.47	0.67	0.75	0.81	0.89	0.95	0.96	0.98
30	–	0.20	–	0.40	0.58	0.65	0.73	0.80	–	0.90	0.95
35	0.08	0.17	0.26	0.34	0.50	0.58	0.64	0.71	–	0.82	0.86
40	–	–	0.22	–	0.44	0.51	0.58	0.69	–	0.74	0.80
45	0.06	0.13	0.20	0.27	0.40	0.41	0.52	0.58	–	0.68	0.73
50	–	0.12	0.18	0.24	0.36	0.41	0.47	0.48	0.58	0.62	0.67

From the results of Table 1 it can be concluded that 20-slot/22-pole combination has the highest winding factors among other combinations.

Double layer windings compared with single layer windings have shorter end windings, more sinusoidal back-EMF, lower rotor losses because of lower magnetic motive force (MMF) space harmonic and support many slot/pole combinations [3]. According to all the conditions connected to a fraction slot winding, double layer FSCW 20-slot/22-pole configuration is considered for designing a five-phase surface-mounted permanent-magnet machine.

The initial design of the machine according to the correlation between the machine design specification and the machine geometrical dimensions based on an analytical method is presented in this part. The geometry of a permanent-magnet motor is mainly determined on the basis of torque capability requirements. Other criteria affecting the motor dimensioning are the motor speed rating, and the minimum rotor critical speed. The desired output power of the motor to be designed is 1100 W at a base speed of 1500 rpm; thus, the rated torque to be reached is about 7 Nm.

The first harmonic of the air gap magnetic flux density B_{g1} is [26]:

$$B_{g1} = \frac{1}{\pi} \int_{-0.5\alpha i\pi}^{0.5\alpha i\pi} B_g \cos \alpha \, d\alpha = \frac{2}{\pi} B_g \sin \frac{\alpha i \, \pi}{2}, \tag{1}$$

where: the coefficient α_i is named the pole-shoe arc-to-pole-pitch ratio, B_g is the magnetic flux density of the air gap.

The rotor outer diameter R_{ro} is calculated as:

$$R_{ro} = \frac{pBgNi}{\pi\sigma}, \tag{2}$$

where: p is the number of magnet pole pairs, σ is shear stress, Ni stands for the coils' ampere-turns and g is the air-gap thickness.

The air-gap thickness g for $p > 1$ (number of magnet pole pairs) should be expressed as [26]:

$$g = 0.18 + 0.006P^{0.4}, \tag{3}$$

where P is the output power in watt.

The peak value of the stator (armature) line current density (A/m) or specific electric loading A_m is given by [26]

$$A_m = \frac{2m\sqrt{2}NI_a}{\pi D_{sin}} = \frac{m\sqrt{2}NI_a}{p\tau} = \frac{m\sqrt{2}NJ_aS_a}{p\tau}, \tag{4}$$

where: D_{sin} is the stator inner diameter, J_a is the current density in the stator (armature) conductors (A/m²), N is the number of armature turns per phase, I_a is the armature current, τ is the pole pitch, s_a is the cross section of armature conductors including parallel wires and m is the number of parallel paths.

The physical size of the motor is formulated as a function of the flux density in the air gap B_g, in the tooth B_t, and in the back iron B_{bi}. The back-iron thickness h_{bi} is calculated as [26]:

$$h_{bi} = \frac{B_g \pi D_{sin}}{2B_{bi}2p} . \tag{5}$$

The tooth height h_t is expressed as a function of external diameter D_{sout} and internal diameter D_{sin} as [26]:

$$h_t = \frac{D_{sout} - D_{sin}}{2} - h_{bi}.$$ (6)

Then the tooth width b_{tb} is calculated as [26]:

$$b_{tb} = \frac{B_g \pi D_{sin} L}{B_t Q L},$$ (7)

where Q is the number of slots, and L is the stack length.

The slot area S_{slot} is expressed as [26]:

$$S_{slot} = \frac{\pi}{4Q} \left[(D_{sout} - 2h_{bi})^2 - D_{sin}^2 \right] - b_{tb} h_t.$$ (8)

The number of turns per coil N_{coil} for double-layer winding is given by [26]

$$N_{coil} = \frac{1}{2} \frac{J_c S_{slot} K_{sf}}{I_R},$$ (9)

where: S_{slot} is the slot area, K_{sf} is the slot fill factor, I_R is the rms phase current.

The volume of all permanent magnets used in a motor calculated by Equation (10), [26].

$$V_M = 2p h_M w_M l_M,$$ (10)

where h_M, w_M and l_M are the height, width, and length of the PM, respectively.

Considering all the flux generated by the permanent magnet is linked with a stator winding, the fundamental component of back EMF can be calculated by [26]

$$E = 4.44 f N_c B_1 K_{w1} \frac{2}{\pi} \frac{\pi D}{p} L,$$ (11)

where: B_1 is the first harmonic of the air gap magnetic flux density, f is the frequency, N_c is the number of turns per phase and K_{w1} is the fundamental winding factor, D is the stator bore, L is the active length of the motor.
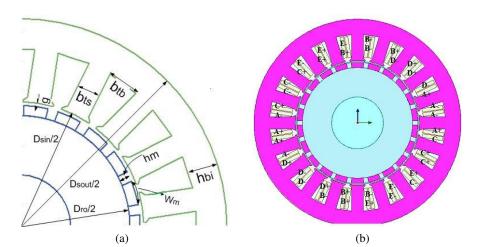
The electromagnetic torque is formulated as [3]:

$$T_d = \frac{Selm \cos \psi}{2\pi ns} = \frac{\pi}{4} K_w D_{sin}^2 L B_g A_m \cos \psi,$$ (12)

where K_w is the winding factor. Fig. 1(a) indicates a cross-section of a PM motor with its geometrical dimensions.

Some of more significant considerations for the design of an electric motor are the current density restriction, and the motor temperature limitation, maximum flux densities in the stator teeth and back iron. With regard to the motor concerns and the design considerations, the initial design of the motor, according to the analytical relations, was investigated. The designed five-phase motor with 20-slots and 22-poles is shown in Fig. 1(b).

The motor parameters derived from the analysis are shown in Table 2 and the analytical results are listed in Table 3.

(a)   (b)

Fig. 1. Cross-section of the designed SPMSM (a); the five-phase SPMSM motor with 20-slots/22-poles (b)

Table 2. Machine key design parameters

Quantity	Values of the five-phase motor	Symbol
Outer diameter of stator	128.324 (mm)	D_{sout}
Active length	94.895 (mm)	L
Air gap	0.7 (mm)	g
Thickness of magnet	3.56 (mm)	h_m
Pole arc to pole pitch ratio (percent)	82%	y_a
Inner diameter of stator	74.428 (mm)	D_{sin}
Slot depth	15.431 (mm)	h_t
Stator back iron depth (mm)	13.15	h_{bi}
Type of magnet	NdFe35	–
Type of steel	M19_24 G	–
Terminal resistance	2.495 (ohm)	R
Wire diamete	0.5106 (mm)	d
Number of conductors per slot	198	N
Parallel branches	2	m

As we can see from Table 3, the values of the electric loading and armature current density of the machine are reasonable. It can be concluded that the results of the initial design of the machine are in an acceptable range. But the total loss is high and the efficiency of the machine is under 90 percent. Also, the total mass of the machine is relatively high. In the next part for developing the performance of the machine a multi-objective optimization will be done.

Table 3. Initial design results

Quantity	Values of the five-phase motor
Maximum back-EMF	146.583 (V)
Armature thermal load	112.736 (A^2/mm^3)
Linear current density	17.5201 (A/mm)
Armature current density	6.72008 (A/mm^2)
Iron-core loss	27.837 (W)
Armature copper loss	120.268 (W)
Total loss	148.091 (W)
Output power	1100.21 (W)
Input power	1248.552 (W)
Efficiency	88.10 (%)
Rated torque	7.00416 (N·m)
Total mass	6.75 (kg)
Torque density	1.037

3. Optimization

In this section optimization for the designed five-phase motor is done. The design variables are determined as the magnet depth, air gap length, pole arc to pole pitch ratio, active length, depth of tooth base, and the depth of stator back-iron. The variation range of the variables are shown in Table 4. The first purpose of this paper is to maximize torque density considering constraints. The objective function is:

$$G_1(d) = \frac{T_{em}}{W_s + W_m + W_c}, \tag{13}$$

where: d is the vector of variables to be explored, T_{em} is the electromagnetic torque, W_s, W_m, W_c are the weight of used steel, magnets and copper, respectively.

The second objective is to maximize the efficiency subject to considering constraints.

$$G_2(d) = \frac{P}{P_s + P_r + P_c + P}, \tag{14}$$

where: P_c indicates the core loss which consists of hysteresis loss (P_h) and eddy current loss (P_{edd}), P_r denotes the resistive loss in the machine and P_s is the semiconductor loss.

Due to guarantee the suitable performance of the machine, a few of the constraints on the design are considered. The first limitation is concerned to the machine geometry, it is interested to determine the length of the teeth acceptable compared to their width. The current density of the wire is the second constraint that should not increase from a reasonable value. The third constraint is the permanent magnet demagnetization. The tooth flux density must be lower than

the maximum allowable value of the tooth flux density, this is the forth constraint and the same constraints must be considered for the stator back iron and the rotor. All of the constraint functions is introduced as:

$$M(d) = \prod_{i=1}^{N} M_i(D),$$ (15)

where $M(d)$ is the constriants function and N is the number of constraints. M is equal to 1 when all constraints are satisfied and it is equal to 0 as one or more constraints fail to be satisfied. Actually, it is interested to investigate the tradeoff between torque density and efficiency. The fitness function is defined as:

$$G(d) = \begin{bmatrix} G_1(d) \\ G_2(d) \end{bmatrix} M(d),$$ (16)

where $G_1(d)$ and $G_2(d)$ are indicated by (13) as well as (14), respectively, and $M(d)$ is defined by (15). Multi-objective evolutionary algorithms (EAs) that employ traditional genetic algorithms have been abolished because of their:

1) high computational complexity of non-dominated sorting (where the number of objectives and the population size are);
2) non-elitism approach;
3) the need for specifying a sharing parameter.

In this paper, a non-dominated sorting-based multi-objective EA (MOEA), called non-dominated sorting genetic algorithm II (NSGA-II) is used, which moderates all the above three drawbacks. Simulation results on optimization show that the employed NSGA-II is able to find much better spread of solutions and better convergence near the true Pareto-optimal front. The optimization is planned for a population size of 250 over 250 generations. The first step for the optimization is determining design variables and a range for each of them. These ranges are specified depend on the design specifications and the motor design constraints. Table 4 depicts the design variables and ranges for this study.

Table 4. Design variables ranges

Quantity	Min	Max	Symbol
Air gap (mm)	0.3	1	g
Magnet depth (mm)	1	5	h_m
Pole arc to pole pitch ratio (percent)	40	100	y_a
Active length (mm)	20	120	L
Stator back iron depth (mm)	5	30	h_{bi}
Depth of tooth base (mm)	1	25	h_t

In the multi-objective technique, all objective functions are optimized at the same time by determining the design parameters. The Genetic Algorithm technique is effectively employed as a powerful method for multi-objective optimization of permanent-magnet machines [27]. This

algorithm consists of initialization, evaluation, selection, cross-over and mutation. An initial population is produced randomly or according to expert data in the first step.

Over an optimization objective function, the fitness of each individual in this population is inspected. For choosing the parents a selection method is employed to the initial population. A new population is generated by applying the genetic operators to parents. To avoid ignoring elite individuals in each population elitist rules are also used. This method is repeated until optimal parameter quantities are reached. In this paper the objectives are to maximize torque density and the efficiency of the machine, subject to considering constraints.

3.1. Optimization results

The multi-objective optimization is used to optimize two objectives at the same time. This causes a set of so-called *Pareto* optimal results. Fig. 2(a) shows the result of the multi-objective optimization between torque density and efficiency for the five-phase motor.
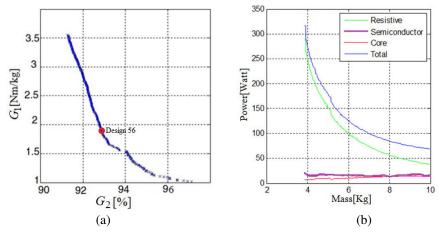

Fig. 2. Pareto-optimal front result for the five-phase motor (a); power loss components versus mass for the five-phase motor (b)

For the designed five phase motor, it is observed that, as the torque torque density changes from 3.5 to 1 the efficiency increases from 90 to 96 percent. Loss components versus mass are shown in Fig. 2(b) Stator resistance loss decreases remarkably with mass but, semiconductor loss and core loss are approximately steady as mass changes. In fact, the conductor mass goes up as the total mass increases. Based on requirements and limitations in motor applications one of the optimized designs must be selected. Due to aircraft and electric vehicle applications, torque and mass of the used electrical motor are two main factors, the 56th design was selected for next studies. The optimized variables and the design results of the 56th design of the pareto-optimal front are listed in Table 5 and Table 6, respectively. It is observed that the specific electric loading and the armature current density of the selected design are in acceptable values. The core loss and armature copper loss are decreased. Also, it is viewed that the efficiency is increased by about five percent and the torque density is increased by about thirty percent. Therefore, proper multi-objective optimization is applied.

Table 5. The optimazed design variables

Quantity	Value	Symbol
Air gap (mm)	0.545	g
Magnet depth (mm)	0.315	h_m
Pole arc to pole pitch ratio (percent)	85	y_a
Active length (mm)	91.15	L
Stator back iron depth (mm)	11.41	h_{bi}
Depth of tooth base (mm)	13.19	h_t

Table 6. Pareto-optimal front results

Quantity	Values of the five-phase motor
Maximum back-EMF	148.146 (V)
Armature thermal load	99.819 (A^2/mm^3)
Linear current density	19.812 (kA/m)
Armature current density	5.021 (A/mm^2)
Iron-core loss	11.8379 (W)
Armature copper loss	72.268 (W)
Outer diameter of stator	120.32 (mm)
Inner diameter of stator	72.42 (mm)
Number of conductors per slot	180
Parallel branches	2
Total loss	84.578 (W)
Output power	1100.11 (W)
Input power	1184.578 (W)
Efficiency	92.86 (%)
Rated torque	7.141 (Nm)
Total mass	5.151 (kg)
Torque density	1.359

4. Numerical modelling of PMSM motor

The initial design was performed depending on the analytical equations of the electric machine. In this section a finite-element analysis was employed to verify the model accuracy. A comparison

was done to verify the optimized variables of the machine concluded from the analytical method and the FEM model.

4.1. Back-EMF

Transient simulation with MAXWELL-2D is done to calculate back-emf of the optimized motor when the rotor has its rated speed (1500 rpm). As we can see in Fig. 3, due to slot/pole combination, it was selected properly, the back-EMF waveforms are completely sinusoidal and their harmonics are eliminated remarkably. The results show acceptable agreement between the analytical calculations and FEM method. The FFT analysis of the back-EMF waveforms of the five-phase motor is shown in Fig. 4. It is observed that the back-EMF of the five-phase motor has satisfactory harmonics analysis.
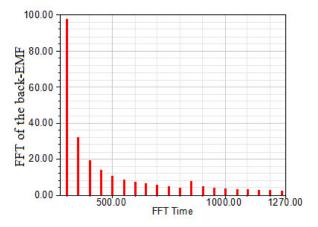
Fig. 3. Back-EMF calculations at rated speed

Fig. 4. FFT analysis of the back-EMF waveform of the five-phase motor

4.2. Electromagnetic torque

The electromagnetic torque of a five-phase motor during a full-load condition for the analytical design and the FEA method is shown in Fig. 5, the average torque of the five phase motor is 7.2 Nm. It should be considered that the analytical design method only implements the fundamental of the air-gap magnetic field and thus the resulting torque is an average value without pulsations. However, this average agrees with the average value of the FEA method.
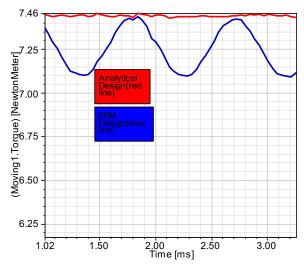

Fig. 5. Electromagnetic torque of the five-phase SPMSM motor

Finite element analysis results are employed to validate the optimized motor. The results are depicted in Table 7. From the results, it is understood that the inaccuracy is below 5% and it is concluded that the FEM method confirms the accuracy of the optimized design.

Table 7. Optimum design results for five- phase motor

Quantity	Analytical	FEM
Output power (W)	1100.11	1100.05
Output torque (Nm)	7.141	7.014
Total loss (W)	84.578	88.231
Total mass (kg)	5.151	5.672
Machine efficiency	92.86%	92.57%
Torque density	1.359	1.234

4.3. Thermal analysis of the designed machine

It is essential to have enough information about the temperature distribution in the motor. An FEA is a reliable thermal analysis tool for electrical motors. The thermal distribution of the

optimized five-phase motor is shown Fig. 6. For the designed SPMSM operation, the main heat sources are the stator copper loss and the stator core loss. As we can see from Table 8 all parts of the optimized motor are operating in acceptable temperature.
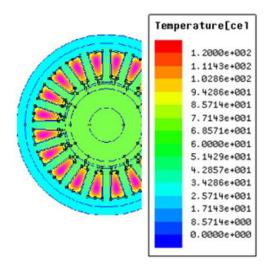

Fig. 6. The thermal distribution of the optimized five- phase motor

Table 8. The result of thermal analysis of the designed five- phase motor

Part	Temp [°C]
Rotor	98.3
Winding slot	119.7
Stator yoke	105.9
Stator teeth	107.5

4.4. Prototype and experiment

The optimized FSCW five-phase, surface-mounted PM machine with 20-slot/22-pole is prototyped and tested for validation. The rotor with 22 poles, the stator core with the windings and the prototyped machine are shown in Fig. 7.

At first, the winding inductance of each machine phase is measured by using a LCR meter. In addition, DC phase resistance is measured. The maesurments compared to the resistance and inductance values are calculated during the intial design of the machine (Table 9). The higher value of the resistance can be observed due to the fact that the prototype machine has larger end-windings than expected and the measured phase inductance is 5 percent lower than expected.

To measure the back-EMF, the machine phase windings are connected in star form and the test is done for a number of speeds, ranging from 0 to 1500 rpm. Fig. 8 shows the experimental

Fig. 7. Rotor core, stator core with windings and prototyped machine

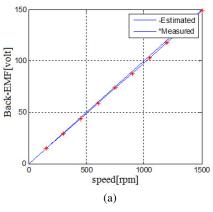Table 9. Comparison between measured and estimatated resistance and inductance

Part	Measured	Estimated
Resistance (ohm)	2.156	1.99
Inductance (mH)	14.126	14.834

setup. A comparison between the estimated and measured back-EMF at different speed is shown in Fig. 9(a). It can be seen that the obtained results are highly reasonable. The small differences between the estimated and measured results are due to a number of reasons, like different characteristics of the used PM and iron materials as well as manufacturing tolerances.

Fig. 8. Experimental setup

The experimental back-EMF of the prototyped machine at a rated speed of 1500 rpm is shown in Fig. 9(b). It could be concluded that the value and waveform of lab the measured back-EMF of the prototype five-phase machine are approximately the same as theoretical measurements.
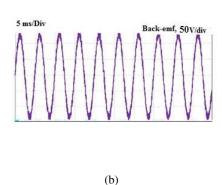
(a)   (b)

Fig. 9. Comparison between estimated and measured back-EMF at different (a); the experimental back-EMF of the prototyped machine at a rated speed of 1500 rpm (b)

5. Conclusions

In this paper, a five-phase surface-mounted permanent-magnet motor was designed and optimized, also the advantages of a multi-phase motor over a three-phase motor were investigated. To optimize the designed motors, a multi-objective optimization based on a genetic algorithm method was used. To evaluate the performance of the optimized machine, the 2D-FEM was applied. It was concluded that the analytical model confirms the accuracy of the design, also it was shown that a multi-phase motor can produce higher electromagnetic torque and back-EMF and lower cogging torque compared with the three-phase motor.

References

[1] Gang L., Bo R., Zi Q., *Design guidelines for fractional slot multi-phase modular permanent magnet machines*, IET Electric Power Application, vol. 11, no. 6, pp. 1023–1031 (2017).

[2] Listwan J., *Analysis of fault states in drive systems with multi-phase induction motors*, Archives of Electrical Engineering, vol. 68, no. 4, pp. 817–830 (2019).

[3] EL-Refaie A.M., *Fractional-Slot Concentrated-Windings Synchronous Permanent Magnet Machines: Opportunities and Challenges*, IEEE Transactions on Industrial Electronics, vol. 57, no. 1, pp. 107–121 (2010).

[4] Caramia R., Piotuch P., Pałka R., *Multi-objective FEM based optimization of BLDC motor using Matlab and Maxwell scripting capabilities*, Archives of Electrical Engineering, vol. 63, no. 1, pp. 115–124 (2014).

[5] Sarikhani A., Mohammed O., *Multiobjective design optimization of coupled PM synchronous motor-drive using physics-based modeling approach*, IEEE Transactions on Magnetics, vol. 47, no. 5, pp. 1266–1269 (2011).

[6] Cros J., Viarouge P., *Synthesis of high performance PM motors with concentrated windings*, IEEE Transactions on Energy Conversion, vol. 17, no. 2, pp. 248–253 (2002).

[7] Zhu Z., Howe D., *Instantaneous magnetic field distribution in brushless permanent magnet motors, part III: Effect of stator slotting*, IEEE Transactions on Magnetics, vol. 29, no. 1, pp. 143–151 (1993).

[8] Proca A., Keyhani A., El-Antably A., Lu W., Dai M., *Analytical model for permanent magnet motors with surface mounted magnets*, IEEE Transactions on Energy Conversion, vol. 18, no. 3, pp. 386–391 (2003).

[9] Refaie A.M., Jahns T.M., Novotny D.W., *Analysis of surface permanent magnet machines with fractional slot concentrated windings*, IEEE Transactions on Energy Conversion, vol. 21, no. 1, pp. 34–43 (2006).

[10] EL-Refaie A.M., Jahns M., *Optimal flux weakening in surface PM machines using fractional slot concentrated windings*, IEEE Transactions on Industry Applications, vol. 41, no. 3, pp. 790–800 (2005).

[11] Chen J., Zhu Z., *Winding configurations and optimal stator and rotor pole combination of flux-switching PM brushless AC machines*, IEEE Transactions on Energy Conversion, vol. 25, no. 2, pp. 293–302 (2010).

[12] Yong K., Hong C., Chang K., Pan S., *A back EMF optimization of double layered large-scale BLDC motor by using hybrid optimization method*, IEEE Transactions on Magnetics, vol. 47, no. 5, pp. 998–1001 (2011).

[13] Sadeghi S., Parsa L., *Multiobjective Design Optimization of Five-Phase Halbach Array Permanent-Magnet Machine*, IEEE Transactions on Magnetics, vol. 47, no. 6, pp. 828–837 (2011).

[14] Islam S., Islam R., Sebastian T., *Experimental Verification of Design Techniques of Permanent-Magnet Synchronous Motors for Low-Torque-Ripple Applications*, IEEE Transactions on Industry Applications, vol. 47, no. 1, pp. 28–37 (2011).

[15] Li Y., Xing J., Wang T., Lu Y., *Programmable Design of Magnet Shape for Permanent Magnet Synchronous Motors With Sinusoidal Back EMF Waveforms*, IEEE Transactions on Magnetics, vol. 44, no. 9, pp. 18–25 (2008).

[16] Parasiliti F., Villani M., Lucidi S., *Finite-Element-Based Multiobjective Design Optimization Procedure of Interior Permanent Magnet Synchronous Motors for Wide Constant-Power Region Operation*, IEEE Transactions on Magnetics, vol. 6, no. 10, pp. 211–219 (2012).

[17] Lim D., Kyung Y., Sang J., *Optimal Design of an Interior Permanent Magnet Synchronous Motor by Using a New Surrogate-Assisted Multi-Objective Optimization*, IEEE Transactions on Magnetics, vol. 51, no. 11, pp. 11–19 (2015).

[18] Parsa L., Toliyat A., *Five-Phase Interior Permanent-Magnet Motors With Low Torque Pulsation*, IEEE Transactions on Industry Applications, vol. 43, no. 1, pp. 128–137 (2007).

[19] Cassimere B., Sudhoff D., *Population based design of surfacemounted permanent magnet synchronous machines*, IEEE Transactions on Energy Conversion, vol. 24, no. 2, pp. 41–48 (2009).

[20] Deb K., *Multi-Objective Optimization Using Evolutionary Algorithms*, Wiley (2001).

[21] Kim J., Cho D., Jung H., Lee C., *Niching genetic algorithm adopting restricted ompetition selection combined with pattern search method*, IEEE Transactions on Magnetics, vol. 38, no. 2, pp. 1001–1004 (2002).

[22] Fatima M., Seifeddine B., *Analysis, simulation and experimental strategies of 5-phase permanent magnet motor control*, Archives of Electrical Engineering, vol. 68, no. 3, pp. 629–641 (2019).

[23] Zheng P., Sui Y., Zhenxing F., *Investigation of a Five-Phase 20-Slot/18-Pole PMSM for Electric Vehicles*, 17th International Conference on Electrical Machines and Systems, Hangzhou, China, pp. 22–25 (2014).

[24] Sudhoff D., Cale J., Cassimere N., Swinney D., *Genetic algorithm design of a permanent magnet synchronous machine*, in Proc. IEEE International Conference Electrical Machines and Drives, New York, US, pp. 1011–1019 (2005).

[25] Sudhoff D., Lee Y., *Energy Systems Analysis Consortium (ESAC) Genetic Optimization System Engineering Tool (GOSET) Version 1.05 Manual*, School of Electrical and Computer Engineering, Purdue Univ., West Lafayette (2003).

[26] Hendershot M., Miller J., *Design of Brushless Permanent Magnet Motors*, Monographs in Electrical and Electronic Engineering, Oxford University Press (1995).

[27] Di Barba P., Mognaschi M., Venini P., Wiak S., *Biogeography-inspired multi-objective optimization for helping MEMS synthesis*, Archives of Electrical Engineering, vol. 66, no. 3, pp. 607–62 (2017).